

# Synthesis and Biologic Evaluation of $^{11}\text{C}$ -Methyl-D-Glucoside, a Tracer of the Sodium-Dependent Glucose Transporters

Guy M. Bormans, PhD<sup>1</sup>; Griet Van Oosterwyck, MSc<sup>1</sup>; Tjibbe J. de Groot, PhD<sup>1</sup>; Maike Veyhl, PhD<sup>2</sup>; Luc Mortelmans, MD<sup>1</sup>; Alfons M. Verbruggen, PhD<sup>1</sup>; and Hermann Koepsell, MD<sup>2</sup>

<sup>1</sup>Laboratory of Radiopharmaceutical Chemistry, Faculty of Pharmaceutical Sciences, and Department of Nuclear Medicine, University of Leuven, Leuven, Belgium; and <sup>2</sup>Institute of Anatomy and Cell Biology, Bayerische Julius-Maximilians-Universität, Würzburg, Germany

This study aimed to synthesize and to evaluate the biologic characteristics of  $^{11}\text{C}$  labeled methyl-D-glucoside, a nonmetabolizable tracer that is selectively transported by sodium-dependent glucose transporters (SGLTs). **Methods:**  $^{11}\text{C}$ -Methyl-D-glucoside was prepared by methylation of glucose with  $^{11}\text{C}$ -methyl triflate and was obtained as a mixture of anomers that were separated with high-performance liquid chromatography. The biodistribution of both the D- and L-isomers was determined in mice, and the presence of metabolites in the blood was investigated. The intrarenal distribution of  $^{11}\text{C}$ -methyl-D-glucoside in mouse kidneys was visualized using autoradiography. Transport of  $\alpha$ -methyl-D-glucoside and  $\beta$ -methyl-D-glucoside by the human sodium-D-glucose cotransporter hSGLT1 was characterized after expression of hSGLT1 in oocytes of *Xenopus laevis*. **Results:** The developed preparation procedure provided  $^{11}\text{C}$ -methyl-D-glucoside in a total synthesis time of 20 min and a yield of 30% (decay corrected). The  $\alpha$ - and  $\beta$ -anomers of methyl-D-glucoside were reabsorbed from the primary urinary filtrate and showed only a minimal urinary excretion. Because methyl-L-glucoside was not reabsorbed and the reabsorption of methyl-D-glucoside was blocked by phlorizin, sodium-D-glucose cotransporters were critically involved.  $\beta$ -Methyl-D-glucoside was accumulated in the kidneys to a higher extent than the  $\alpha$ -anomer, suggesting that the basolateral efflux from the tubular cells is slower for the  $\beta$ -anomer. Autoradiography showed that methyl-D-glucoside was accumulated throughout the renal cortex, suggesting that both sodium-D-glucose cotransporters expressed in kidney, SGLT1 and SGLT2, are involved in the uptake. The tracer was found to be metabolically stable and did not accumulate in red blood cells, which indicates that methyl-D-glucoside is not transported by the sodium-independent transporter GLUT1. Electrical measurements in *Xenopus* oocytes revealed that  $\alpha$ -methyl-D-glucoside and  $\beta$ -methyl-D-glucoside are transported by the human SGLT1 transporter with similar maximal transport rates and apparent Michaelis-Menten constant values. **Conclusion:**  $^{11}\text{C}$ -

Methyl-D-glucoside is a selective tracer of sodium-dependent glucose transport and can be used to visualize the function of this transporter with PET in vivo.

**Key Words:** sodium-dependent glucose transporter; methylglucoside; PET;  $^{11}\text{C}$

**J Nucl Med 2003; 44:1075–1081**

**T**he phospholipid bilayer of plasma membranes is virtually impermeable for polar compounds such as glucose. The permeation of glucose through these biologic membranes is achieved by transporters of 2 distinct protein families termed GLUT and SGLT (1–3). Seven isoforms of the GLUT transporters have been identified that mediate passive diffusion of glucose or fructose. Three isoforms of the sodium-D-glucose cotransporters (SGLTs) have been identified. The SGLTs are able to concentrate glucose within cells because these transporters couple D-glucose uptake with the inwardly directed gradient of sodium that is maintained by the sodium-potassium pump at the expense of adenosine triphosphate. SGLT1 is a high-affinity transporter that is expressed on the apical side of epithelial cells in the small intestine and in the S3 segment of renal proximal tubules. SGLT1 transports sodium and D-glucose with a stoichiometry of 2:1. The isoform SGLT2 is a low-affinity glucose transporter that is expressed in the S1 and S2 segments of renal proximal tubules and transports sodium and glucose with a 1:1 stoichiometry (1). The properties of SGLT3 appear to vary largely between different species. For example, SGLT3 from pig is a low-affinity sodium-D-glucose cotransporter with an activity and sodium:glucose stoichiometry similar to that of SGLT1 (4), whereas human SGLT3 does not contribute significantly to sodium-D-glucose cotransport (H. Koepsell, unpublished data, 2002). SGLT1 is also expressed in bovine brain arteries (5) and in neurons of the central nervous system (6).

Received May 2, 2002; revision accepted Sep. 20, 2002.

For correspondence or reprints contact: Guy M. Bormans, PhD, Laboratory of Radiopharmaceutical Chemistry, Universitaire Ziekenhuizen Gasthuisberg, Herestraat 49, B-3000 Leuven, Belgium.

E-mail: guy.bormans@uz.kuleuven.ac.be

The SGLT transporters exhibit important physiologic functions and are regulated in a tissue-specific manner. In small intestine, SGLT1 is upregulated by luminal glucose (7), whereas in confluent cells of the renal epithelial cell line LLC-PK<sub>1</sub>, SGLT1 is downregulated when the glucose concentration in the medium is increased (8). Similarly, sodium-D-glucose cotransport in cultured bovine brain endothelial cells is upregulated by hypoglycemia (9), and sodium-D-glucose cotransport in neurons is upregulated after induction of an epileptic seizure that may also lead to a depletion of D-glucose (6). Genetic defects of the SGLT1 and SGLT2 result in glucose-galactose malabsorption (10) or familial renal glycosuria (11), respectively. SGLT1 may be used as a target for drugs or as a diagnostic marker. For example, transcription of SGLT1 has been observed in several tumor cell lines and various human carcinomas (12,13) so that the accumulation of a labeled SGLT substrate in these tumors could be used for their identification. It has been shown that the decrease of  $\alpha$ -methyl-D-glucoside uptake in isolated proximal tubules caused by exposure to xenobiotics correlates with the nephrotoxicity of the xenobiotics (14). Currently, compounds that inhibit SGLT transporters are explored for the treatment of noninsulin-dependent diabetes mellitus with the aim to increase the urinary excretion of excess plasma glucose (15).

GLUT and SGLT transporters exhibit specific differences in glucose recognition. For example the presence of a hexapyranose ring with an equatorial C2 hydroxyl group is a prerequisite to have a high affinity for SGLT1 (16). Thus, deoxy-D-glucose and FDG that lack the C2 hydroxyl group are not good substrates for SGLT1. This explains why, in contrast to glucose, FDG is excreted in the urine because only about 50% of FDG in the glomerular filtrate is reabsorbed in the proximal tubule (17). Alkylglucosides are substrates for SGLT transporters and are poorly transported or not transported by GLUT transporters (18,19). The affinity of alkylglucosides for SGLT1 increases with the alkyl chain length, but only methyl-, ethyl-, and propylglucosides are translocated, whereas the longer chain compounds are competitive, nontransported inhibitors (18). In this study we have synthesized <sup>11</sup>C-labeled  $\alpha$ -methyl-D-glucoside ( $\alpha$ MDG) and  $\beta$ -methyl-D-glucoside ( $\beta$ MDG) to provide a nonmetabolizable radiotracer that enables the *in vivo* visualization of the SGLT function with PET. We evaluated the biodistribution and urinary excretion of  $\alpha$ MDG and  $\beta$ MDG in mice and compared the transport properties of these compounds by human SGLT1.

## MATERIALS AND METHODS

All reagents and solvents were obtained commercially from Aldrich, Acros, or Merck unless otherwise specified. <sup>11</sup>CO<sub>2</sub> was produced by proton bombardment of N<sub>2</sub> (containing 1% O<sub>2</sub>) with 10-MeV protons in a cyclotron (Cyclone 10/5; Ion Beam Applications).  $\alpha$ -Methyl-D-<sup>14</sup>C-glucopyranoside (11 GBq/mmol) was obtained from Amersham Buchler. The chemicals used for RNA synthesis were obtained as described (20).

## Radiosynthesis and HPLC Separation

<sup>11</sup>C-Methyl triflate was obtained by passage of <sup>11</sup>C-CH<sub>3</sub>I over a Ag-triflate column at 180°C. <sup>11</sup>C-CH<sub>3</sub>I was synthesized from <sup>11</sup>CO<sub>2</sub> that was first reduced to <sup>11</sup>CH<sub>4</sub> and subsequently reacted with I<sub>2</sub> vapor at 650°C using a home-built recirculation synthesis module. <sup>11</sup>C-Methyl triflate was bubbled through a solution of 3 mg of D-glucose (or L-glucose) in a mixture of 0.5 mL of 0.05 mol/L NaOH and 1 mL of acetone for 5 min at room temperature. The solution was then neutralized with 0.2 mL phosphate buffer, pH 6 (0.5 mol/L), and acetone was evaporated by heating (90°C) under a stream of helium over 4 min. The resulting solution was diluted with saline to an appropriate radioactive concentration for the biodistribution study with the mixture of  $\alpha$ - and  $\beta$ -anomers of <sup>11</sup>C-methylglucoside.

For biodistribution of the individual  $\alpha$ - and  $\beta$ -anomers, the anomeric mixture was separated using high-performance liquid chromatography (HPLC) with an Aminex HPX-87c column (Bio-Rad) (300 × 7.8 mm) eluted with water at a flow rate of 0.5 mL/min. The  $\alpha$ - and  $\beta$ -anomers of <sup>11</sup>C-methyl-D-glucoside were found to coelute with authentic  $\alpha$ -MDG (retention time [Rt] = 9.7 min) and authentic  $\beta$ MDG (Rt = 8.7 min), respectively. The isolated peaks were reanalyzed 60 min after isolation by the same HPLC system. The purified  $\alpha$ - and  $\beta$ -anomers were diluted with saline to an appropriate radioactive concentration for the biodistribution studies. Plasma was analyzed on a carbohydrate-NH<sub>2</sub> column (300 × 4.1 mm; Alltech) eluted with a mixture of CH<sub>3</sub>CN:H<sub>2</sub>O (90:10) at a flow rate of 1.5 mL/min. In this system both anomers elute as 1 peak at Rt = 4.8 min.

The column eluates were passed through a refractive index and a radiometric detector, and the detector signals were processed using a Rachel acquisition system (LabLogic). The recovery of radioactivity in the eluate (relative to the injected activity) was 98%.

## Biodistribution in Mice and Autoradiography

The biodistribution experiments were performed in compliance with national laws related to the conduct of animal experimentation. Male NMRI mice (body mass, 25–30 g; fed ad libitum) were sedated by intramuscular injection of 0.05 mL of a 1:4 diluted solution of Hypnorm (fentanylcitrate [0.315 mg/mL] and fluanisone [10 mg/mL]; Janssen Pharmaceutica). Then, 0.1 mL of the tracer solution (3.7 MBq) was injected in each of 4 mice via a tail vein. For pretreatment with phlorizin, sedated mice were injected intraperitoneally with 800 mg of phlorizin/kg of body mass. Phlorizin was dissolved to a concentration of 200 mg/mL in 1,3-propanediol and was injected 1 h before the tracer.

The mice were killed by decapitation at 10 or 30 min after injection. Blood was collected in a tared tube and weighed. All organs and other body parts were dissected and their radioactivity was determined in a  $\gamma$ -counter (Wizard 1480; Wallac). Corrections were made for background radiation and physical decay during counting. For calculation of total blood activity, blood mass was assumed to be 7% of body mass. The hematocrit value of a blood sample obtained 30 min after injection was determined by centrifugation of a hematocrit microcapillary for 5 min in a dedicated centrifuge (Damon). A blood sample (about 1 mL) was weighed and counted for radioactivity. The sample was centrifuged for 10 min at 1,500g and plasma was pipetted off, weighed, and counted in a  $\gamma$ -sample changer. Four-tenths milliliter of the plasma sample was added to 1.5 mL of acetonitrile to denature the plasma proteins. The sample was centrifuged and the supernatant was filtered through a 0.22- $\mu$ m membrane filter and injected on an HPLC column. The HPLC eluate was collected in 1-mL fractions and their radioactivity was determined in a  $\gamma$ -counter.

The activity associated with the denaturated plasma proteins in the sediment obtained after centrifugation was also determined by counting in a  $\gamma$ -counter.

To determine the *in vivo* intrarenal distribution, 0.1 mL of a saline solution containing 37 MBq of  $^{11}\text{C}$ -methyl-D-glucoside (mixture of isomers) was injected intravenously in a sedated NMRI mouse. The animal was killed by decapitation at 30 min after injection and a kidney was rapidly removed and immediately frozen in 2-methylbutane (cooled to  $-25^\circ\text{C}$  with liquid nitrogen). Serial frozen coronal sections of 50  $\mu\text{m}$  were cut and mounted on microscope slides. The sections were immediately air dried at  $50^\circ\text{C}$  and exposed for 2 h to a high-performance storage phosphor screen (Packard) that was scanned in a Phosphor Imager scanner (Cyclone; Packard).

### Expression of hSGLT1 in *Xenopus laevis* Oocytes and Transport Measurements

To prepare sense complementary RNA (cRNA) of human SGLT1 (21), purified pBluescript II plasmid containing hSGLT1 was linearized with *EcoRI* and 5'-7meGppp5'-G capped cRNA was synthesized by T3 RNA polymerase (20). The cRNAs were extracted twice with phenol/chloroform/isoamyl alcohol (25:24:1), precipitated with acidic ethanol, and dissolved in double-distilled water treated with diethylpyrocarbonate.

For expression, *Xenopus* oocytes were defolliculated and injected with 50 nL of water per oocyte without or with 10 ng of hSGLT1-cRNA (20). The oocytes were incubated 3 d at  $19^\circ\text{C}$  in Ori buffer (5 mmol/L Hepes-Tris, pH 7.4, 100 mmol/L NaCl, 3 mmol/L KCl, 2 mmol/L  $\text{CaCl}_2$ , 1 mmol/L  $\text{MgCl}_2$ ) to which 50 mg/L gentamycin was added.

For tracer flux measurements of  $\alpha\text{MDG}$  in *Xenopus* oocytes, the oocytes were incubated in the absence or presence of 100  $\mu\text{mol/L}$  phlorizin with Ori buffer (room temperature) containing 10  $\mu\text{mol/L}$   $^{14}\text{C}$ - $\alpha\text{MDG}$  plus different concentrations of  $\beta\text{MDG}$ . After a 1-h incubation, the oocytes were washed and radioactivity in the oocytes was analyzed as described (20). The electric properties of glucose uptake were investigated using the 2-microelectrode voltage-clamp technique (22). The oocytes were clamped to  $-50$  mV and continuously perfused at room temperature ( $\sim 3$  mL/min) with Ori buffer. Different concentrations of  $\alpha\text{MDG}$  or  $\beta\text{MDG}$  were added to the buffer, and the inward current induced by cotransported sodium was measured.

The uptake of  $^{14}\text{C}$ - $\alpha\text{MDG}$  was calculated as the difference of the uptake in 7–10 oocytes in the absence of phlorizin and the uptake in 7–10 oocytes in the presence of phlorizin per data point. Mean values  $\pm$  SE values are presented. The apparent inhibitory constant ( $K_i$ ) for  $\beta\text{MDG}$  inhibition of  $^{14}\text{C}$ - $\alpha\text{MDG}$  uptake was calculated by fitting the Michaelis–Menten equation to the data. The electrical measurements were performed with at least 4 oocytes from 2 different oocyte batches. The Michaelis–Menten equation was fitted to the currents that were induced by different glucose concentrations.

## RESULTS

### Radiosynthesis

The reaction of glucose with  $^{11}\text{C}$ -methyl triflate in alkaline conditions yields not only  $^{11}\text{C}$ -methylglucoside but also  $^{11}\text{C}$ -methanol as a side product. The latter is easily removed by evaporation after neutralization of the reaction mixture.

The described production method yields a mixture of 2 anomers that coelute during HPLC analysis with the authentic  $\alpha$ - and  $\beta$ -anomers of methyl-D-glucoside, respectively (detected with a refractive index detector). Reanalysis of the HPLC-isolated individual anomers showed that they do not interconvert in aqueous solution, in agreement with literature data (23). The anomers of  $^{11}\text{C}$ -methyl-D-glucoside are obtained in a ratio of 25%  $\alpha$ -anomer and 75%  $\beta$ -anomer. This ratio was not influenced by changes in the reaction conditions (concentration of NaOH, glucose, reaction temperature, reaction duration). The amount of radiochemical impurities in the final solution was  $<5\%$ . The overall synthesis procedure (starting from  $^{11}\text{CO}_2$ ) takes 30 min and provides  $^{11}\text{C}$ -methylglucoside with a decay-corrected yield of 30% (relative to starting  $^{11}\text{C}$ - $\text{CO}_2$ ). Because of the low sensitivity of the refractive index detector, the specific activity could not be calculated but can be assumed to be in the same range (20 GBq/ $\mu\text{mol}$ ) as that of other  $^{11}\text{C}$  tracers that were synthesized using the same methylation module. The mixture of anomers of  $^{11}\text{C}$ -methyl-L-glucoside was obtained using an identical synthesis procedure but starting from L-glucose.

### Biodistribution in Mice and Autoradiography

The biodistribution of the standard preparation that contained a mixture of the  $\alpha$ - and  $\beta$ -anomers of  $^{11}\text{C}$ -methyl-D-glucoside was investigated in mice at 10 and 30 min after injection (Table 1). The kidney is the organ with the highest concentration of  $^{11}\text{C}$ -methyl-D-glucoside, and the activity accumulating in the kidneys still continues to increase up to 30 min after injection. In mice pretreated with phlorizin, the renal accumulation of  $^{11}\text{C}$ -methyl-D-glucoside observed at 30 min after injection was inhibited by 78% compared with normal mice. In the absence of phlorizin, the clearance from blood and carcass was slow, and only a small amount of  $^{11}\text{C}$ -methyl-D-glucoside was excreted with the urine. However, after pretreatment with phlorizin the urinary excretion at 30 min after injection of the tracer was increased about 4-fold and a lower percentage of the injected dose was observed in the blood as compared with the nonpretreated animals. The data indicate that transport systems that can be inhibited by phlorizin are required for renal accumulation and reabsorption of  $^{11}\text{C}$ - $\alpha\text{MDG}$  or  $^{11}\text{C}$ - $\beta\text{MDG}$ . A more detailed analysis of the blood at 30 min after injection showed that  $>98\%$  of the activity in blood was associated with plasma but was not bound to proteins (protein binding,  $<1\%$ ). This indicates that  $^{11}\text{C}$ - $\alpha\text{MDG}$  or  $^{11}\text{C}$ - $\beta\text{MDG}$  is poorly transported or not transported by the passive glucose transporter GLUT1, which is expressed in erythrocytes (1). Also, the low brain uptake observed for methyl-D-glucoside at both 10 and 30 min after injection is in agreement with poor transport by GLUT1. HPLC analysis of the plasma indicated that all  $^{11}\text{C}$  is in the chemical form of methylglucoside, excluding significant degradation or metabolism of  $^{11}\text{C}$ -methyl-D-glucoside during the experiment.

Table 2 presents separate results of the biodistribution studies 30 min after intravenous injection of the individual  $\alpha$ - and

**TABLE 1**  
Biodistribution in Normal Mice and Mice Pretreated with Phlorizin (800 mg/kg) After Intravenous Injection of <sup>11</sup>C-Methyl-D-Glucoside (Mixture of Anomers)

Biodistribution	10 min after injection		30 min after injection		30 min after injection (pretreatment with phlorizin)	
	%ID	%ID/g	%ID	%ID/g	%ID	%ID/g
Urine	1.13 ± 0.54		2.35 ± 0.69		9.11 ± 13.03	
Kidneys	21.23 ± 3.83	22.21 ± 6.05	25.97 ± 4.74	29.82 ± 2.14	5.76 ± 1.83	10.10 ± 2.67
Liver	10.40 ± 0.82	4.59 ± 0.85	10.08 ± 1.44	4.26 ± 0.48	9.77 ± 1.35	5.17 ± 0.42
Spleen	0.45 ± 0.27	1.86 ± 0.14	0.30 ± 0.15	2.38 ± 0.20	0.41 ± 0.09	2.84 ± 0.38
Lungs	1.71 ± 0.36	4.77 ± 0.66	1.27 ± 0.05	4.62 ± 0.33	1.48 ± 0.67	5.40 ± 1.14
Heart	0.45 ± 0.05	2.05 ± 0.25	0.56 ± 0.07	2.32 ± 0.25	0.48 ± 0.05	3.07 ± 0.57
Intestines	5.85 ± 0.44	1.36 ± 0.24	5.51 ± 0.61	1.44 ± 0.10	8.54 ± 1.77	2.33 ± 0.46
Stomach	0.66 ± 0.07	0.86 ± 0.32	1.21 ± 0.47	1.47 ± 0.49	1.12 ± 0.33	2.13 ± 0.54
Cerebrum	0.09 ± 0.01	0.27 ± 0.03	0.08 ± 0.02	0.25 ± 0.04	0.19 ± 0.04	0.63 ± 0.15
Cerebellum	0.04 ± 0.02	0.36 ± 0.06	0.04 ± 0.02	0.35 ± 0.06	0.09 ± 0.04	0.93 ± 0.22
Blood	17.73 ± 1.44	5.32 ± 0.67	17.24 ± 0.94	5.11 ± 0.22	14.31 ± 2.87	6.21 ± 1.27
Carcass	50.04 ± 4.14	1.37 ± 0.17	45.62 ± 4.54	1.21 ± 0.15	54.08 ± 10.69	2.19 ± 0.42

%ID = percentage of injected dose.  
Values are mean ± SD (n = 4).

β-anomers of <sup>11</sup>C-methyl-D-glucoside. A higher accumulation in the kidneys was observed for the β-anomer compared with the α-anomer. This corresponds to a lower concentration of the β-anomer in blood and carcass 30 min after intravenous injection. Due to the effective reabsorption in the kidney, the urinary excretion of <sup>11</sup>C-αMDG and <sup>11</sup>C-βMDG is low. The urinary excretion is somewhat higher for the β-anomer that is accumulated in proximal tubular cells. The data suggest that the second step in transtubular movement of <sup>11</sup>C-methyl-D-glucoside (the basolateral efflux from cell to interstitium, which is supposed to be mediated by the passive glucose transporter GLUT2 (2)) is slower for the β-anomer compared with the α-anomer.

For a mixture of α- and β-anomers of methyl-L-glucoside, a 20–40 times higher excretion into urine was observed compared with the α- and β-anomers of methyl-D-glucoside. This indicates that both methyl-D-glucoside anomers are reabsorbed from the glomerular filtrate in contrast to the anomers of methyl-L-glucoside. Because the renal accumulation of methyl-L-glucoside was low, it may be concluded that methyl-L-glucoside was not accepted as a substrate of the sodium-D-glucose cotransporters SGLT1 and SGLT2 that are localized in renal brush border membranes. The results of the biodistribution study suggest that the renal accumulation of methyl-D-glucoside represents its accumulation in proximal tubular cells. Both the α- and

**TABLE 2**  
Biodistribution in Mice After Intravenous Injection of <sup>11</sup>C-αMDG, <sup>11</sup>C-βMDG, and <sup>11</sup>C-Methyl-L-Glucoside (Mixture of Isomers)

Biodistribution	<sup>11</sup> C-αMDG, 30 min after injection		<sup>11</sup> C-βMDG, 30 min after injection		<sup>11</sup> C-Methyl-L-glucoside,* 30 min after injection	
	%ID	%ID/g	%ID	%ID/g	%ID	%ID/g
Urine	0.88 ± 0.56		2.26 ± 0.09		42.70 ± 1.51	
Kidneys	8.46 ± 1.00	11.25 ± 1.72	31.28 ± 8.06	35.16 ± 11.95	7.09 ± 3.00	8.94 ± 2.11
Liver	11.31 ± 1.24	4.93 ± 0.06	8.38 ± 0.64	3.90 ± 0.88	8.12 ± 0.90	4.40 ± 0.59
Spleen	0.70 ± 0.46	2.18 ± 1.41	0.55 ± 0.07	1.91 ± 0.73	0.70 ± 0.10	2.28 ± 0.50
Lungs	1.75 ± 0.24	5.27 ± 0.32	1.07 ± 0.17	3.89 ± 1.27	0.87 ± 0.19	3.43 ± 0.68
Heart	0.49 ± 0.12	3.24 ± 0.86	0.44 ± 0.04	1.82 ± 0.73	0.39 ± 0.12	2.15 ± 0.56
Intestines	7.47 ± 0.31	1.96 ± 0.38	5.90 ± 0.75	1.31 ± 0.37	5.13 ± 0.37	1.58 ± 0.18
Stomach	1.31 ± 0.48	1.92 ± 0.59	0.50 ± 0.70	0.79 ± 0.77	0.54 ± 0.47	1.13 ± 0.88
Blood	19.22 ± 1.81	6.78 ± 0.32	12.45 ± 2.41	4.51 ± 1.39	6.68 ± 1.14	2.68 ± 0.57
Carcass	59.43 ± 2.53	1.94 ± 0.10	42.76 ± 6.25	1.49 ± 0.25	31.25 ± 3.75	1.08 ± 0.14

\*Mixture of α- and β-anomers.  
%ID = percentage of injected dose.  
Values are mean ± SD (n = 4).

$\beta$ -anomers may be transported into the cell, but the  $\beta$ -anomer may be released more slowly at the basolateral site, resulting in a higher renal accumulation and a lower concentration in blood.

The intrarenal distribution of the anomeric mixture of  $^{11}\text{C}$ -methyl-D-glucoside was determined by autoradiography on a coronal kidney slice obtained 30 min after injection (Fig. 1). An accumulation of activity was observed throughout the renal cortex reaching into the outer medulla. SGLT2 is expressed in S1 and S2 segments of renal proximal tubules in the outer cortex and midcortex and SGLT1 is expressed in S3 segments of renal proximal tubules that are localized in the inner cortex and outer medulla. Therefore, these data strongly suggest that  $^{11}\text{C}$ -methyl-D-glucoside is transported by both SGLT1 and SGLT2.

#### Transport of $\alpha\text{MDG}$ and $\beta\text{MDG}$ by Human SGLT1

To evaluate the potential human use of  $^{11}\text{C}$ -methyl-D-glucoside with PET, we compared the transport of  $\alpha\text{MDG}$  and  $\beta\text{MDG}$  mediated by the human SGLT1 (hSGLT1) transporter. *Xenopus* oocytes expressing hSGLT1 were clamped to  $-50$  mV, and inward currents that were induced after incubation of  $\alpha\text{MDG}$  or  $\beta\text{MDG}$  in the presence of 100 mmol/L sodium were measured. The current traces in Figure 2A were obtained when the same oocyte was first incubated with 5 mmol/L  $\alpha\text{MDG}$  and then incubated with 5 mmol/L  $\beta\text{MDG}$ . Because maximal currents were induced with these substrate concentrations (see below), they were used to compare the maximal transport velocities for  $\alpha\text{MDG}$  and  $\beta\text{MDG}$ . Figure 2B shows that hSGLT1 translocates both anomers with similar maximal transport velocities. In Figure 3 the substrate dependence of inward currents by  $\alpha\text{MDG}$  and  $\beta\text{MDG}$  were compared at  $-50$  mV. For both anomers, similar apparent Michaelis-Menten constant values were obtained:  $1.06 \pm 0.03$  mmol/L for  $\alpha\text{MDG}$  and  $0.84 \pm 0.23$  mmol/L for  $\beta\text{MDG}$ . The affinity of  $\beta\text{MDG}$  to hSGLT1 was also determined by tracer flux measurements with 10  $\mu\text{mol/L}$   $^{14}\text{C}$ - $\alpha\text{MDG}$ , which were performed

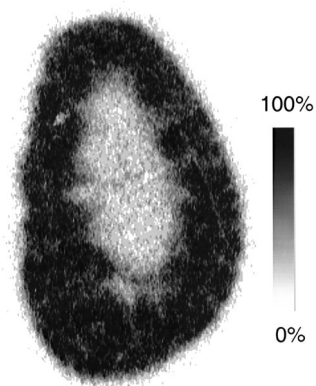


**FIGURE 1.** Intrarenal distribution of  $^{11}\text{C}$ -methyl-D-glucoside at 30 min after injection. Autoradiographic image of 50- $\mu\text{m}$ -thick coronal kidney slice is shown. Image is scaled to maximum pixel intensity of image.

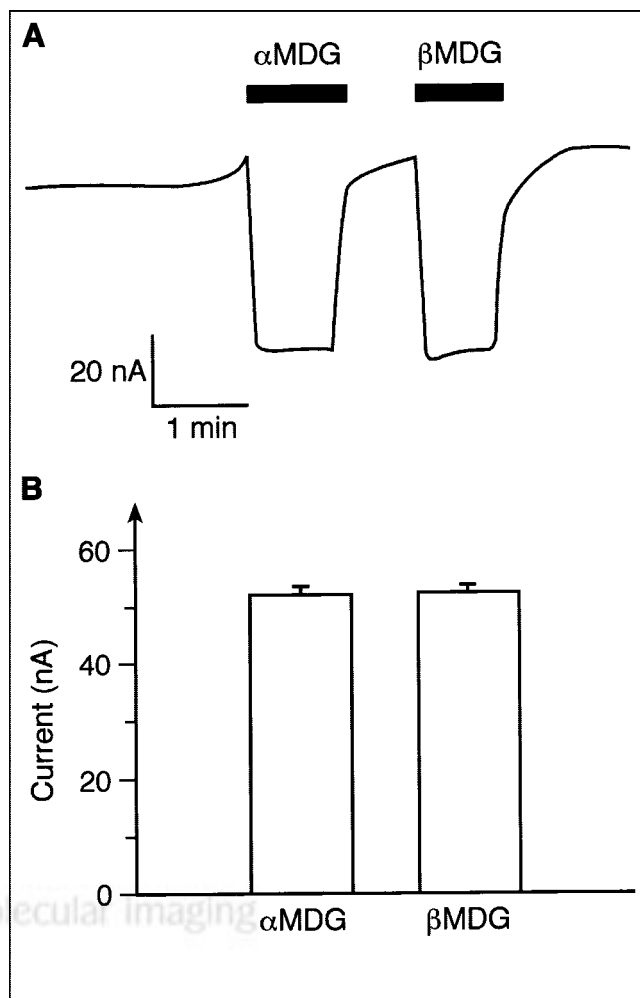


**FIGURE 2.** Comparison of inward currents by hSGLT1 that were induced by saturating concentrations of  $\alpha\text{MDG}$  or  $\beta\text{MDG}$ . *Xenopus* oocytes expressing hSGLT1 were clamped at  $-50$  mV, incubated with Ori buffer without sugar or with Ori buffer containing 5 mmol/L  $\alpha\text{MDG}$  or 5 mmol/L  $\beta\text{MDG}$ , and induced inward currents were measured. (A) Typical current trace from 1 oocyte is shown. (B) Data from 5 experiments are summarized.

with varying concentrations of  $\beta\text{MDG}$  (Fig. 4). A 50% inhibitory concentration of  $0.75 \pm 0.12$  mmol/L was obtained, which represents a  $K_i$  value of 0.74 mmol/L, assuming competitive inhibition. The data show that hSGLT1 transports  $\alpha\text{MDG}$  and  $\beta\text{MDG}$  with the same transport rate and affinity.

#### DISCUSSION

A simple, rapid and robust procedure for the preparation of highly pure  $^{11}\text{C}$ -methyl-D-glucoside that can be used for clinical PET investigations has been developed. The preparation procedure can be easily adapted for production of clinical doses. With this protocol,  $\alpha$ - and  $\beta$ -anomers of methyl-D-glucoside were obtained with a respective relative ratio of 25:75. Urinary excretion and biodistribution in mice were determined for a mixture of  $^{11}\text{C}$ - $\alpha\text{MDG}$  and  $^{11}\text{C}$ -

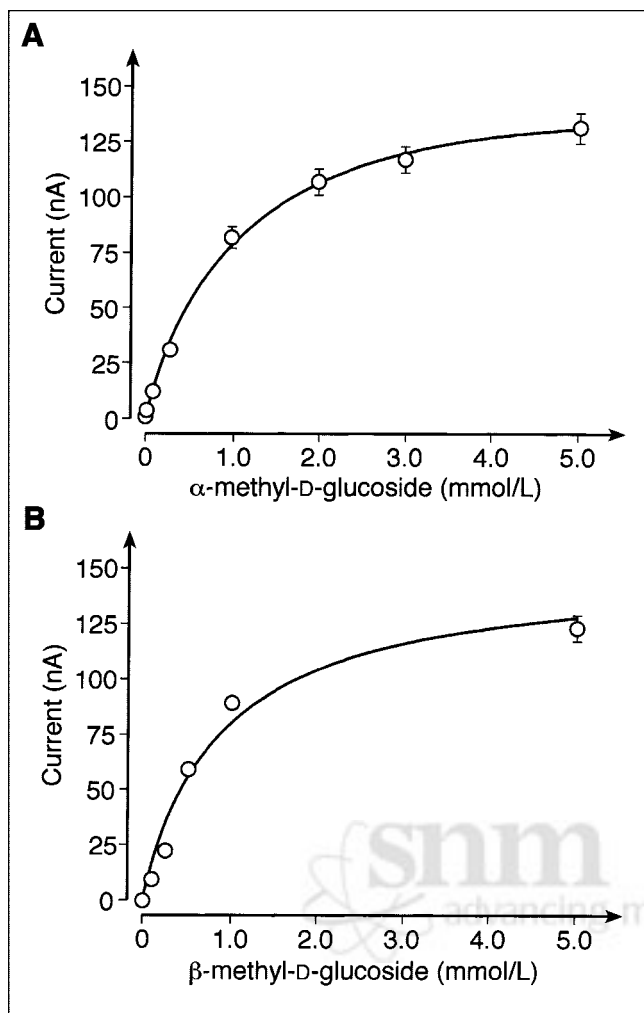


**FIGURE 3.** Substrate dependence of hSGLT1-expressed inward currents induced by  $\alpha$ MDG or  $\beta$ MDG. *Xenopus* oocytes were clamped at  $-50$  mV, incubated with Ori buffer containing different concentrations of  $\alpha$ MDG (A) or  $\beta$ MDG (B), and glucose-induced currents were measured. Mean values  $\pm$  SD from 4 oocytes are presented. Michaelis-Menten equation was fitted to data.

$\beta$ MDG, for  $^{11}\text{C}$ - $\alpha$ MDG or  $^{11}\text{C}$ - $\beta$ MDG separately, and for a mixture of  $\alpha$ - and  $\beta$ - $^{11}\text{C}$ -methyl-L-glucosides. The absence of urinary excretion showed that both  $\alpha$ - and  $\beta$ -methyl-D-glucoside anomers were nearly completely reabsorbed from the primary glomerular filtrate. The reabsorption is stereospecific and depends critically on the activity of sodium-D-glucose cotransport systems (SGLTs) in the brush border membrane of renal proximal tubules because  $^{11}\text{C}$ -methyl-L-glucoside shows extensive urinary excretion. Moreover, urinary excretion of  $^{11}\text{C}$ -methyl-D-glucoside was induced by pretreatment of the animals with phlorizin, a specific inhibitor of the SGLT transporters (24). Consistent with the higher urinary excretion, the accumulation in the kidney observed for  $^{11}\text{C}$ -methyl-D-glucoside was reduced by about 80% when the animals were pretreated with phlorizin and was about 75% lower for  $^{11}\text{C}$ -methyl-L-glucoside. A pro-

nounced accumulation of  $^{11}\text{C}$ -methyl-D-glucoside in the kidneys was observed for the  $\beta$ -anomer and the mixture of  $\alpha$ - and  $\beta$ -anomers, however, not with  $^{11}\text{C}$ - $\alpha$ MDG alone. These data indicate significant differences in the efflux of  $\alpha$ - and  $\beta$ -methyl-D-glucoside anomers across the basolateral membrane of renal proximal tubules.  $\beta$ MDG accumulates in the kidney to a higher extent as basolateral efflux is slower. Our data indicate that the renal accumulation of  $^{11}\text{C}$ -methyl-L-glucoside represents radioactivity in proximal tubular cells rather than in the renal interstitium. The autoradiogram in Figure 1 indicates that  $^{11}\text{C}$ -methyl-D-glucoside accumulated throughout the entire renal cortex and in the outer stripe of the outer renal medulla. Because SGLT2 is expressed in the S1 and S2 segments of renal proximal tubules that are mainly localized in the outer part of the renal cortex whereas SGLT1 is expressed in the S3 segments that are localized in the deep cortex and outer stripe, it can be concluded that  $^{11}\text{C}$ -methyl-D-glucoside is transported into proximal tubular cells by both SGLT1 and SGLT2. Taken together, the anomeric mixture of  $^{11}\text{C}$ -methyl-D-glucoside can be used to visualize the proximal tubular cells that are intact enough to express functionally active sodium-D-glucose cotransporters. Although SGLT1 is also expressed at the brush border membrane of the intestine, no accumulation of  $^{11}\text{C}$ -methyl-D-glucoside was found in this tissue. This can be expected because, after intravenous administration, only a negligible amount of  $^{11}\text{C}$ -methyl-D-glucoside is presented to the intestinal lumen.

We attempted to evaluate the applicability of  $^{11}\text{C}$ -MDG for PET investigations in humans by comparing the transport properties of human SGLT1 for the  $\alpha$ - and  $\beta$ -anomers. Because both anomers are transported with similar apparent

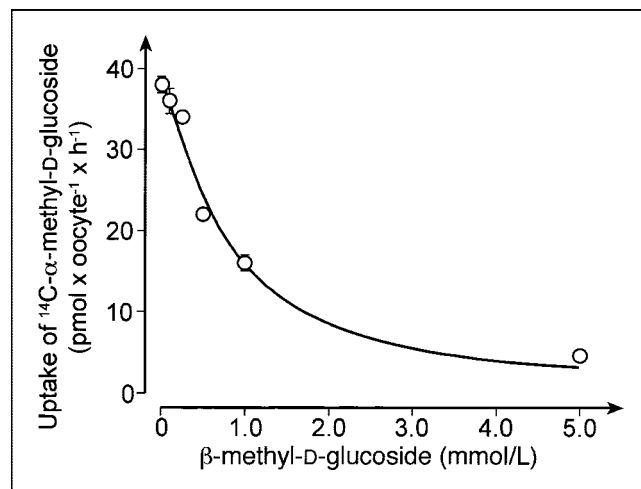


**FIGURE 4.** Inhibition of hSGLT1-expressed uptake of  $^{14}\text{C}$ - $\alpha$ MDG uptake by  $\beta$ MDG. *Xenopus* oocytes expressing hSGLT1 were incubated for 1 h with Ori buffer without and with  $100$   $\mu\text{mol/L}$  phlorizin that contained  $10$   $\mu\text{mol/L}$  of  $^{14}\text{C}$ - $\alpha$ MDG plus indicated concentrations of  $\beta$ MDG. Mean values  $\pm$  SD of phlorizin-inhibited uptake rates measured from pairs of 7–10 oocytes are presented. Michaelis-Menten equation was fitted to data.

Michaelis constant ( $K_m$ ) values and maximum velocity ( $V_{max}$ ) values, the mixture of anomers may be used. PET investigations with  $^{11}\text{C}$ -methyl-D-glucoside may become a valuable diagnostic tool to evaluate local defects in renal nephron function. For example, it could be used to determine the region in which a lobar artery stenosis or a renal tumor leads to damage of the tubular system. It could also be used to monitor the inhomogeneous regeneration of the tubular system after an acute renal failure.

The biodistribution study of  $\alpha$ - and  $\beta$ - $^{11}\text{C}$ -methyl-D-glucoside showed no significant accumulation of activity in other organs, including brain. We previously demonstrated SGLT1 expression in neurons and showed that intravenously injected  $^{14}\text{C}$ - $\alpha$ MDG was increased in the focus of an epileptic seizure that was induced by penicillin (6). Under normal conditions,  $\alpha$ MDG and  $\beta$ MDG may not pass the capillary endothelium like D-glucose. In contrast to D-glucose,  $\alpha$ MDG and  $\beta$ MDG are not transported by GLUT1, as can be concluded from our observation that neither compound entered erythrocytes that express GLUT1. Within or around an epileptic focus, the situation may be different because the pattern of protein expression may have changed (25). In the blood-brain barrier within an epileptic focus, physiologically significant amounts of a glucose transporter may be expressed, resulting in a local accumulation of methyl-D-glucoside. Candidates are SGLT transporters, GLUT2, or another sodium-independent glucose transporter. Future experiments are necessary to elucidate whether  $^{11}\text{C}$ -methyl-D-glucoside can be used to demonstrate upregulation of sodium-D-glucose transporters in brain during epileptic seizures, hypoglycemia, or hypoxemia.

## CONCLUSION

$^{11}\text{C}$ -Methyl-D-glucoside can be easily prepared as a mixture of the  $\alpha$ - and  $\beta$ -anomers, which can be separated by HPLC. In the kidney, both anomers are reabsorbed in renal proximal tubules. The reabsorption critically depends on the functionality of the sodium-D-glucose cotransporters SGLT2 and SGLT1 in the luminal membrane of renal proximal tubules. Compared with the  $\alpha$ -anomer,  $\beta$ -methyl-D-glucoside is accumulated in the proximal tubular cells of the renal cortex to a higher extent because the efflux rate at the basolateral membrane is different for both compounds. Thus,  $^{11}\text{C}$ -methyl-D-glucoside is a tracer for the in vivo visualization of sodium-D-glucose cotransport activity with PET and provides an interesting tool for the in vivo study of SGLT in kidney malfunction. Future studies must elucidate whether  $^{11}\text{C}$ -methyl-D-glucoside may also be used to detect tumors that express SGLT transporters and to determine the upregulation of SGLT transporters in brain during hypoglycemia or epilepsy.

## ACKNOWLEDGMENT

This research was supported by the National Fund for Scientific Research-Flanders, Belgium.

## REFERENCES

- Bell GI, Burant CF, Takeda J, Gould GW. Structure and function of mammalian facilitative sugar transporters. *J Biol Chem.* 1993;268:19161–19164.
- Hediger MA, Rhoads DB. Molecular physiology of sodium-glucose cotransporters. *Physiol Rev.* 1994;74:993–1026.
- Takata K. Glucose transporters in the transepithelial transport of glucose. *J Electron Microscop (Tokyo).* 1996;45:275–284.
- Diez-Sampedro A, Eskandri S, Wright EM, Hirayama BA.  $\text{Na}^+$ -to-sugar stoichiometry of SGLT3. *Am J Physiol.* 2001;280:F278–F282.
- Nishizaki T, Kammescheidt A, Sumikawa K, Asada T, Okada Y. A sodium- and energy-dependent glucose transporter with similarities to SGLT1-2 is expressed in bovine cortical vessels. *Neurosci Res.* 1995;22:13–22.
- Poppe R, Karbach U, Gambaryan S, et al. Expression of the  $\text{Na}^+$ -D-glucose cotransporter SGLT1 in neurons. *J Neurochem.* 1997;69:84–94.
- Shirazi-Beechey SP, Hirayama BA, Wang Y, Scott D, Smith MW, Wright EM. Ontogenetic development of lamb intestinal sodium-glucose co-transporter is regulated by diet. *J Physiol (Lond).* 1991;437:699–708.
- Korn T, K hlkamp T, Track C, et al. The plasma membrane-associated protein RS1 decreases transcription of the transporter SGLT1 in confluent LLC-PK<sub>1</sub> cells. *J Biol Chem.* 2001;276:45330–45340.
- Nishizaki T, Matsuoka T. Low glucose enhances  $\text{Na}^+$ /glucose transport in bovine brain artery endothelial cells. *Stroke.* 1998;29:844–849.
- Martin GM, Turk E, Lostao MP, Kerner C, Wright EM. Defects in  $\text{Na}^+$ /glucose cotransporter (SGLT1) trafficking and function cause glucose-galactose malabsorption. *Nat Genet.* 1996;12:216–220.
- Scrifer SR, Chesney RW, McInnes RR. Genetic aspects of renal tubular transport: diversity and topology of carriers. *Kidney Int.* 1976;9:149–171.
- Veyhl M, Wagner K, Volk K, et al. Transport of the new chemotherapeutic agent  $\beta$ -D-glucosylisophosphoramide mustard (D-19575) into tumor cells is mediated by the  $\text{Na}^+$ -D-glucose cotransporter SAAT1. *Proc Natl Acad Sci USA.* 1998;95:2914–2919.
- Ishiwaka N, Oguri T, Isobe T, Fujitaka K, Kohno N. SGLT gene expression in primary lung cancers and their metastatic lesions. *Jpn J Cancer Res.* 2001;92:874–879.
- Boogard PJ, Mulder GJ, Nagelkerke JF. Isolated proximal tubular cells from rat kidney as an in vitro model for studies on nephrotoxicity. II. Alpha-methylglucose uptake as a sensitive parameter for mechanistic studies of acute toxicity by xenobiotics. *Toxicol Appl Pharmacol.* 1989;101:144–157.
- Tsujihara K, Hongu M, Saito K, et al.  $\text{Na}^+$ -glucose cotransporter (SGLT) inhibitors as antidiabetic agents. 4. Synthesis and pharmacological properties of 4'-dehydroxyphlorizin derivatives substituted on the B ring. *J Med Chem.* 1999;42:5311–5324.
- Ullrich KJ, Rumrich G, Kl ss S. Specificity and sodium dependence of the active sugar transport in the proximal convolution of the rat kidney. *Pflugers Arch.* 1974;351:35–48.
- Moran JK, Lee HB, Blaufox MD. Optimization of urinary FDG excretion during PET imaging. *J Nucl Med.* 1999;40:1352–1357.
- Ramaswamy K, Bhattacharyya BR, Crane RK. Studies on the transport of aliphatic glucosides by hamster small intestine in vitro. *Biochim Biophys Acta.* 1976;433:32–38.
- Kipp H, Lin JT, Kinne RKH. Interactions of alkylglucosides with the renal sodium/D-glucose cotransporter. *Biochim Biophys Acta.* 1996;1282:124–130.
- Veyhl M, Spangenberg J, P schel B, et al. Cloning of a membrane-associated protein which modifies activity and properties of the  $\text{Na}^+$ -D-glucose cotransporter. *J Biol Chem.* 1993;268:25041–25053.
- Hediger MA, Turk E, Wright EM. Homology of the human intestinal  $\text{Na}^+$ /glucose and *Escherichia coli*  $\text{Na}^+$ /proline cotransporters. *Proc Natl Acad Sci USA.* 1989;86:5748–5752.
- Arndt P, Volk C, Gorboulev V, et al. Interaction of cations, anions, and weak base quinine with rat renal cation transporter rOCT2 compared with rOCT1. *Am J Physiol.* 2001;281:F454–F468.
- Nishikawa T, Suzuki S, Kubo H, Ohtani H. On-column isomerisation of sugars during high-performance liquid chromatography: analysis of the elution profile. *J Chromatogr A.* 1996;720:167–172.
- Koepsell H, Fritsch G, Korn K, Madrala A. Two substrate sites in the renal  $\text{Na}^+$ -D-glucose cotransporter studied by model analysis of phlorizin binding and D-glucose transport measurements. *J Membr Biol.* 1990;114:113–132.
- Gass P. Expression of inducible transcription factors after experimental limbic seizures. *Adv Neurol.* 1999;81:347–355.